

A NEW HYBRID PHOTOVOLTAIC-DIESEL SYSTEM CONTROL SCHEME FOR AN ISOLATED LOAD

Noureddine Hidouri^{1,*}, Taoufik Mhamdi^{2,*}, Samah Hammadi^{3,*} & Lassâad Sbata^{4,*}

¹ Preparatory Engineering Institute of Gafsa, Department of Preparatory Technological Engineering studies, Campus Universitaire Sidi Ahmed Zarrouk - 2112 Gafsa, Tunisia

² Higher Institute of Technological Studies of Kasserine, Department of Electrical Engineering, Kasserine University, Feriana Street, Tunisia

³ Higher Institute of Technological Studies of Gafsa, Department of Electrical Engineering, Campus Universitaire Sidi Ahmed Zarrouk - 2112 Gafsa, Tunisia

⁴ National Engineering School of Gabes, Department of Electrical and Control engineering, Zrig, Gabes 6029, Tunisia

* Research Unit of photovoltaic systems, wind and geothermal, National Engineering School of Gabes, Tunisia

ABSTRACT

In this paper, the Authors present a hybrid photovoltaic-diesel system control. The considered system is composed of a self excited induction generator (SEIG) and a photovoltaic array (PV array) and a supervisor associated to an isolated DC load. The diesel motor is used to drive the SEIG in order to feed an isolated DC load when the PV array required insulation is down. The load receives the input power from the photovoltaic array through a buck converter and a DC bus when the insulation is sufficient; else it receives the required active power from the SEIG through a diode rectifier, LC-LC filter and a DC bus. A modelling study was performed for the proposed Hybrid system components. Modelling of the PV array, SEIG, Diesel engine, rectifier, LC-LC filter, DC bus and buck converter were established and used in the control proposed scheme. The DC bus control aiming to extract the required active power from the hybrid system is studied and analyzed. An extensive simulation work was performed to extract the significant results. To show up the high system performances, presented results are discussed and prove how the proposed methodology is an efficient hybrid photovoltaic diesel control procedure.

Keywords: *Hybrid system, photovoltaic, diesel, SEIG, Buck converter*

1. INTRODUCTION

Electrical energy is an essential factor for the development of human societies. It is one of the fundamental necessities for every day's life which improves our quality and makes daily living more convenient. The shortage of fossil fuel, their unstable prices and the trend to reduce dependency of pollutant energetic sources increase the demand of renewable energy that become viable alternative energy sources for electrical power production in remote area [1,2]. PV energy is now becoming a promising economical renewable energy source since it offers many advantages such as incurring no fuel costs, not being polluting, requiring little maintenance, and emitting no noise, but the output power varies randomly due to fluctuation of solar insulation and climatic conditions. It completely disappears during the night hours. There must be a stand by power source to meet the load energy demand. Diesel engine driven generator are the most common electrical energy production scheme in small and medium size power application is used to provide an uninterrupted energy sources in remote area, it works as a compensator to the fluctuating power output of the photovoltaic array (PVA) [3,4]. That's why the design of hybrid power system has received considerable attention. It may constitute economical solution in many application, and provide more reliable supply of electricity through the combination of several energy sources. A Diesel engine drive a generator to produce electricity. DC and synchronous machine are easy to be controlled but presents expensive costs of installation and operation due to fabrication and maintenance features. The use of induction generator is becoming more and more popular for renewable energy sources. The self excited induction generator SEIG has many advantages, reduced size, rugged and low cost, robust and brushless ruggedness, ease of maintenance, absence of DC power supply for field excitation better transient performance, and self protection the major drawback of SEIG are reactive power consumption, it's relatively poor voltage and frequency regulation. However an autonomous induction machine is able to generate electric power if self excitation occur [5], the capacitor used are connected to the generator in order to compensate the reactive power consumed by the generator. The frequency, the slip, the output voltage and the operating range of the system depend of the characteristics of the induction generator, the value of the capacitor and the diesel engine speed of rotation [6]. The voltage decreases when the load increase for a fixed value of the capacitor, it is difficult to produce smooth voltage regulation, the control of the voltage and frequency of a autonomous PV-diesel system is more challenging than in a large grid [7]. To overcome poor voltage

regulation of the SEIG a number of schemes have been proposed switched capacitors, a saturable reactor, a short shunt and a long shunt configuration. In this paper two control loops are always included to stabilize the voltage frequency and magnitude. The first is the speed diesel engine control to maintain the speed constant, the second is called automatic voltage regulator which works to keep the voltage magnitude constant through the control of the field excitation to make possible the connections of diverse energy sources [3] The design process of hybrid energy systems requires the selection and sizing of the most suitable combination of energy sources. Thus in this paper a supervisor is used to select the suitable energy source when the insulation varies.

2. THE HYBRID SYSTEM MODEL

Related to work published in [16], the proposed hybrid system considered in this work is shown in figure1.

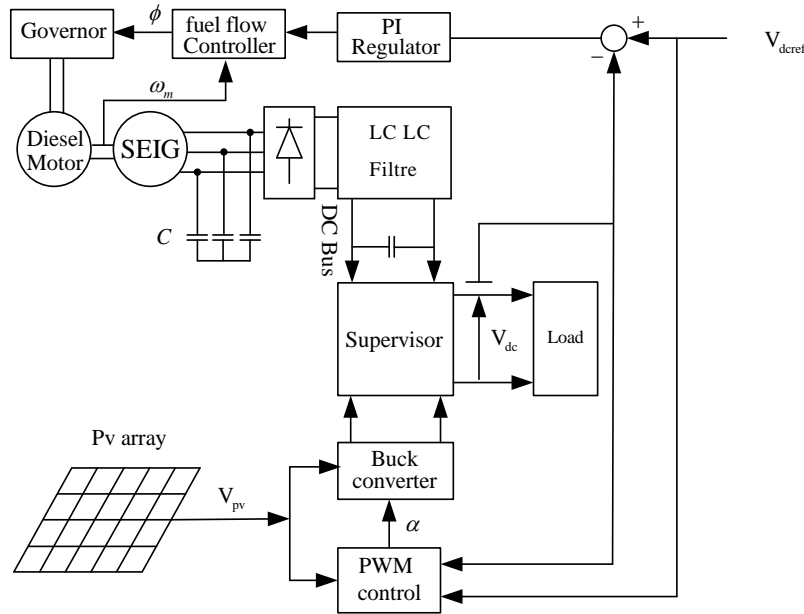


Figure 1. The proposed hybrid system configuration

In order to convert the mechanical power to electrical power required by the load, the rotor of the diesel motor is coupled to a self excited induction generator. The three phase full bridge diode rectifier which is connected to the stator of the SEIG is used to rectify the generated terminal voltage. The main rule of the used LCLC filter is to obtain a smooth DC voltage by suppressing the voltage fluctuation. The obtained DC voltage is used to feed a DC load. In other way, the DC load can be fed also by a DC voltage provided only by the PV panel through the PWM controlled buck converter when the insulation is sufficient. The decision about the chose between the two ways is realised by the supervisor used in this hybrid configuration.

2.1. Cell and PV Models

The solar cell is an electric component that is used for technologically converting the solar energy into electricity to produce the electrical energy needs in some application requirement. In order to prove their research work, many authors proposed different models for the solar cell [8-11]. The electric model of a solar cell is shown in figure 2 where I_{ph} , D , R_{sc} and R_{pc} represent respectively the light-generated current source, the diode, the series and parallel resistances [13,14].

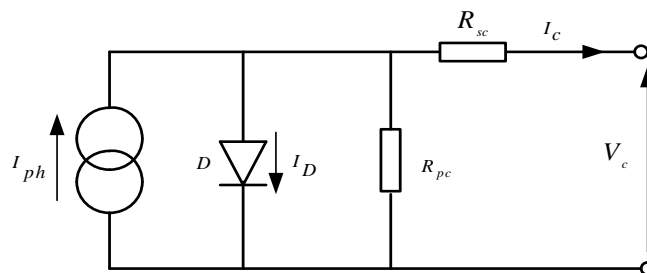


Figure 2. Equivalent solar cell's electric circuit

At the reference condition defined by the cell junction temperature T_{c_ref} and the insulation G_{ref} , the photocurrent I_{ph_ref} is equal to the reverse saturation current I_{sc_ref} .

At the desired cell junction temperature T_c and the insulation G , the cell photocurrent I_{ph} can be deduced from the reference data condition given by equation where K_{SCT} stands for the short circuit current temperature coefficient [9,12,14].

$$I_{ph} = \frac{G}{G_{ref}} \left(I_{sc_ref} + K_{SCT} (T_c - T_{c_ref}) \right) \tag{1}$$

The desired reverse saturation current I_{rs} is also obtained from the reference condition according to relation (2), where E_g , q , k and β represent respectively the band gap energy of the semiconductor, the electron charge, the ideal factor off the solar cell and the boltzman constant [9].

$$I_{rs} = I_{rs_ref} \left(\frac{T_c}{T_{c_ref}} \right)^3 \exp \left[\frac{qE_g}{\beta k} \left(\frac{1}{T_c} - \frac{1}{T_{c_ref}} \right) \right] \tag{2}$$

Many others express the characteristic equation relating the cell's current I_c to its voltage V_c as represented in (3), [8,9].

$$I_c = I_{ph} - I_{rs} \left(\exp \left(\frac{q}{\beta k T_c} (V_c + R_{sc} I_c) \right) - 1 \right) - \frac{(V_c + R_{sc} I_c)}{R_{pc}} \tag{3}$$

The solar panel can be composed of N_p array of modules assembled in parallel; each one can be composed of N_s modules assembled in series. A module can also contain n_s cells associated in series configuration. This consideration expresses the relations between the panel's and the cells parameters, relation (4).

$$\begin{cases} I_p = N_p I_c \\ V_p = n_s N_s V_c \\ R_{sp} = \frac{n_s N_s}{N_p} R_{sc} \\ R_{pp} = \frac{n_s N_s}{N_p} R_{pc} \end{cases} \tag{4}$$

In this consideration, the non-linear characteristic equation related the panel current I_p to its voltage V_p is shown in (5).

$$I_p = N_p I_{ph} - N_p I_{rs} \left(\exp \frac{q}{\beta k T_c} \left(\frac{V_p}{n_s N_s} + \frac{R_{sc} I_p}{N_p} \right) - 1 \right) - \frac{N_p}{R_{pc}} \left(\frac{V_p}{n_s N_s} + \frac{R_{sc} I_p}{N_p} \right) \tag{5}$$

2.2. Buck Converter Model

Figure 3 shows the structure of the PWM buck converter published in [14,15] and used in this research work. As an assumption, the power devices are considered to be ideal. This idea leads to the consideration that when the IGBT is open, the current equals zero, and when it is closed, the voltage is zero as well. Also, both capacitive and inductive losses are neglected.

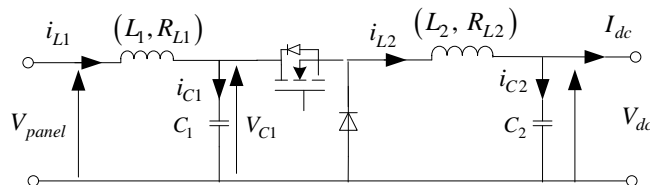


Figure 3. Structure of the used buck converter

The command of the buck-converter depends on the IGBT state that is defined by the PWM signal where α denotes the duty cycle and T denotes the operating period.

Along the operating time period T , the IGBT is switched on for αT and switched off over $(1-\alpha)T$ intervals.

In the state space domain, the buck converter model with respect to the αT interval can be represented by state equations ((6) and (7)):

$$\begin{bmatrix} \dot{i}_{L1} \\ \dot{i}_{L2} \\ \dot{V}_{c1} \\ \dot{V}_{c2} \end{bmatrix} = \begin{bmatrix} -\frac{R_{L1}}{L_1} & 0 & -\frac{1}{L_1} & 0 \\ 0 & -\frac{R_{L2}}{L_2} & \frac{1}{L_2} & -\frac{1}{L_2} \\ \frac{1}{C_1} & -\frac{1}{C_1} & 0 & 0 \\ 0 & \frac{1}{C_2} & 0 & -\frac{1}{R_{Load}C_2} \end{bmatrix} \begin{bmatrix} i_{L1} \\ i_{L2} \\ V_{C1} \\ V_{C2} \end{bmatrix} + \begin{bmatrix} \frac{1}{L_1} \\ 0 \\ 0 \\ 0 \end{bmatrix} V_{panel} \tag{6}$$

$$V_{dc} = [0 \ 0 \ 0 \ 1][i_{L1} \ i_{L2} \ V_{C1} \ V_{C2}]^t \tag{7}$$

In the state space domain, the buck converter model with respect to the $(1-\alpha)T$ interval, is represented by the following state equations ((8) and (9)):

$$\begin{bmatrix} \dot{i}_{L1} \\ \dot{i}_{L2} \\ \dot{V}_{c1} \\ \dot{V}_{c2} \end{bmatrix} = \begin{bmatrix} -\frac{R_{L1}}{L_1} & 0 & -\frac{1}{L_1} & 0 \\ 0 & -\frac{R_{L2}}{L_2} & 0 & -\frac{1}{L_2} \\ \frac{1}{C_1} & 0 & 0 & 0 \\ 0 & \frac{1}{C_2} & 0 & -\frac{1}{R_{Load}C_2} \end{bmatrix} \begin{bmatrix} i_{L1} \\ i_{L2} \\ V_{C1} \\ V_{C2} \end{bmatrix} + \begin{bmatrix} \frac{1}{L_1} \\ 0 \\ 0 \\ 0 \end{bmatrix} V_{panel} \tag{8}$$

$$V_{dc} = [0 \ 0 \ 0 \ 1][i_{L1} \ i_{L2} \ V_{C1} \ V_{C2}]^t \tag{9}$$

During the two intervals previously presented, the converter model is obtained by merging the two state models (eq. (6) and (8)) presented above relatively to the two intervals with respect to the IGBT state. Relatively to the work published in [15] and used in this research work, c designates a Boolean variable that takes the value ($c = 0$) if the IGBT is switched off and the diode is switched on and takes the value ($c = 1$) if the IGBT is switched on and the diode is switched off. According to this idea, the global model taking account of the buck converter switching topology is given as:

$$\begin{bmatrix} \dot{i}_{L1} \\ \dot{i}_{L2} \\ \dot{V}_{c1} \\ \dot{V}_{c2} \end{bmatrix} = \begin{bmatrix} -\frac{R_{L1}}{L_1} & 0 & -\frac{1}{L_1} & 0 \\ 0 & -\frac{R_{L2}}{L_2} & \frac{c}{L_2} & -\frac{1}{L_2} \\ \frac{1}{C_1} & -\frac{c}{C_1} & 0 & 0 \\ 0 & \frac{1}{C_2} & 0 & -\frac{1}{R_{Load}C_2} \end{bmatrix} \begin{bmatrix} i_{L1} \\ i_{L2} \\ V_{C1} \\ V_{C2} \end{bmatrix} + \begin{bmatrix} \frac{1}{L_1} \\ 0 \\ 0 \\ 0 \end{bmatrix} V_{panel} \tag{10}$$

$$V_{dc} = [0 \ 0 \ 0 \ 1][i_{L1} \ i_{L2} \ V_{C1} \ V_{C2}]^t \tag{11}$$

2.3. Diesel engine model

The developed torque C_{de} of the diesel engine can be expressed by relation (12), it depends of the fuel flow (ϕ) adjusted by the governor and the combustion process that introduce a delay time τ_{de} , [3,17,23,24].

$$C_{de} = k_{de} \cdot \phi(p) e^{-\tau_{de} p} \tag{12}$$

The governor is modeled by relation (13) is an electromechanical device that receives a control signal S_{gs} in order to adjust the fuel flow [3,17,18].

$$\phi(p) = \frac{k_g}{1 + \tau_g p} S_{gs} \quad (13)$$

2.4. Self Exited Induction Generator Model

2.4.1. SEIG d-q model

In the Concordia stationary reference frame, when the Ohm's law is applied to the SEIG phasor, the direct and quadratic components of the stator and rotor voltage are respectively given by relations (14) and (15), [20].

$$\begin{cases} v_{sd} = R_s i_{sd} + \frac{d\phi_{sd}}{dt} \\ v_{sq} = R_s i_{sq} + \frac{d\phi_{sq}}{dt} \end{cases} \quad (14)$$

$$\begin{cases} v_{rd} = R_r i_{rd} + \frac{d\phi_{rd}}{dt} + \omega_r \phi_{rq} \\ v_{rq} = R_r i_{rq} + \frac{d\phi_{rq}}{dt} - \omega_r \phi_{rd} \end{cases} \quad (15)$$

The direct and quadratic components of the stator and rotor flux are respectively given by relation (16) and (17), [4,18].

$$\begin{cases} \phi_{sd} = L_s i_{sd} + M_{sr} i_{rd} + \phi_{sd0} \\ \phi_{sq} = M_{rs} i_{rq} + L_s i_{sq} + \phi_{sq0} \end{cases} \quad (16)$$

$$\begin{cases} \phi_{rd} = L_r i_{rd} + M_{sr} i_{sd} + \phi_{rd0} \\ \phi_{rq} = L_r i_{rq} + M_{rs} i_{sq} + \phi_{rq0} \end{cases} \quad (17)$$

The SEIG in its standard form is an induction machine with a capacitor bank across its stator terminals for excitation purpose. The voltage equations (18) in Concordia reference frame can be found from the equivalent circuit given by Figure 4.

$$\begin{bmatrix} V_{Cd} \\ V_{Cq} \\ -\omega_r \phi_{rq0} \\ \omega_r \phi_{rd0} \end{bmatrix} = \begin{bmatrix} R_s + pL_s & 0 & pM_{sr} & 0 \\ 0 & R_s + pL_s & 0 & pM_{sr} \\ pM_{sr} & \omega_r M_{sr} & R_r + pL_r & \omega_r L_r \\ -\omega_r M_{sr} & pM_{sr} & -\omega_r L_r & R_r + pL_r \end{bmatrix} \begin{bmatrix} i_{sd} \\ i_{sq} \\ i_{rd} \\ i_{rq} \end{bmatrix} \quad (18)$$

The electromagnetic torque is given by the following formula:

$$C_{em} = p(i_{sq} \phi_{sd} - i_{sd} \phi_{sq}) \quad (19)$$

The capacitor voltages are equal to the stator voltage, thus the direct and quadratic expression for the capacitor voltages are given by relation (20):

$$\begin{cases} V_{Cd} = v_{sd} = \frac{1}{C} \int i_{Cd} dt + V_{Cd0} \\ V_{Cq} = v_{sq} = \frac{1}{C} \int i_{Cq} dt + V_{Cq0} \end{cases} \quad (20)$$

Figure 4 gives the Concordia model of the SEIG, [6,20,21,26]. The parameters of the SEIG obtained from the test at rated values of voltage and frequency are given by Table 1, [26]. It's essential to indicate that the magnetizing inductance varies with the voltage; this important fact should be taken in consideration for SEIG application. The expression of the magnetizing inductance with consideration of the phase voltage is given by relation (21), [26].

$$M_{sr} = -1.5610 \cdot 10^{-11} v_s^4 + 2.4410 \cdot 10^{-8} v_s^3 - 1.1910 \cdot 10^{-5} v_s^2 + 1.4210 \cdot 10^{-3} v_s + 0.245 \quad (21)$$

The leakage inductances of stator and rotor are given by the following formula:

$$\begin{cases} \ell_s = L_s - M_{sr} \\ \ell_r = L_r - M_{sr} \end{cases} \quad (22)$$

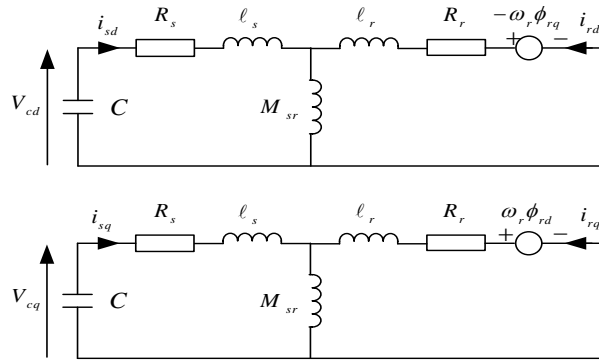


Figure 4. Concordia reference frame SEIG d-q Model

2.4.2. SEIG complex model

In the Concordia stationary reference frame, applied to the machine stator phasor and the rotor phasor, the Ohm’s law is given by:

$$\bar{v}_s = R_s \bar{i}_s + \frac{d\bar{\phi}_s}{dt} \quad (23)$$

$$\bar{v}_r = R_r \bar{i}_r + \frac{d\bar{\phi}_r}{dt} - j\omega_r \bar{\phi}_r \quad (24)$$

The stator flux vector $\bar{\phi}_s$ and the rotor flux vector are linked to the stator current \bar{i}_s and the rotor current \bar{i}_r by equations (25) and (26)

$$\bar{\phi}_s = L_s \bar{i}_s + M_{sr} \bar{i}_r \quad (25)$$

$$\bar{\phi}_r = L_r \bar{i}_r + M_{sr} \bar{i}_s \quad (26)$$

The capacitor voltage vector is equal to the stator voltage vector and expressed by relation (27):

$$\bar{V}_C = \bar{v}_s = \frac{1}{C} \int \bar{i}_c dt + \bar{V}_{C0} \quad (27)$$

With respect relations (23), (24), (25), (26) and (27), the voltage equations (28) in Concordia reference frame can be found from the equivalent circuit given by Figure 5.

$$\begin{bmatrix} \bar{V}_C \\ j\omega_r \bar{\phi}_r \end{bmatrix} = \begin{bmatrix} R_s + pL_s + pM_{sr} & pM_{sr} \\ pM_{sr} & R_r + pL_r + pM_{sr} \end{bmatrix} \begin{bmatrix} \bar{i}_s \\ \bar{i}_r \end{bmatrix} \quad (28)$$

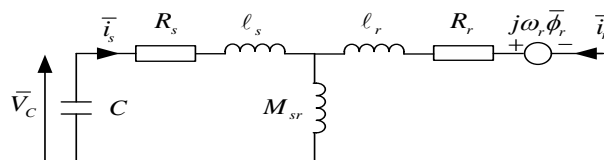


Figure 5. Concordia reference frame SEIG Complex Model

2.4. Diode rectifier model

The three phase full bridge rectifier is supplied by a three phase voltage of The SEIG given by:

$$\begin{cases} v_{s1} = v_m \sin(\omega_0 t) \\ v_{s2} = v_m \sin(\omega_0 t - \frac{2\pi}{3}) \\ v_{s3} = v_m \sin(\omega_0 t - \frac{4\pi}{3}) \end{cases} \quad (29)$$

The output voltage of the full bridge rectifier can be expressed by (30), [22]:

$$v_{rec} = \max(v_{s1}, v_{s2}, v_{s3}) - \min(v_{s1}, v_{s2}, v_{s3}) \tag{30}$$

The operation laws of a full bridge three phase 6-diodes rectifier fed with a three phase voltage source:

$$V_{rec0} = \frac{3\sqrt{6}}{2\pi} v_{sM} = 1.654 v_{sM} \tag{31}$$

2.5. LCLC Filter model

A well designed filter can eliminate voltage fluctuation and suppress the high frequency harmonics to improve the power quality. The state model of the used LCLC filter given by figure 6 is given by the relation (32) , [16]:

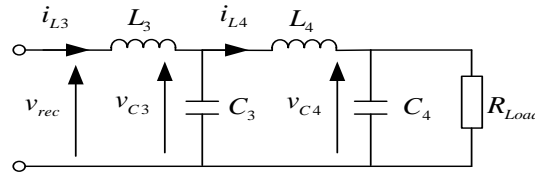


Figure 6. LCLC filter structure

$$\begin{cases} \frac{di_{L3}}{dt} = \frac{v_{rec}}{L_3} - \frac{v_{C3}}{L_3} \\ \frac{di_{L4}}{dt} = \frac{v_{C3}}{L_4} - \frac{v_{C4}}{L_4} \\ \frac{dv_{C3}}{dt} = \frac{i_{L3} - i_{L4}}{C_3} \\ \frac{dv_{C4}}{dt} = \frac{i_{L4}}{C_4} - \frac{v_{C4}}{R_{Load}C_4} \end{cases} \tag{32}$$

In the state space domain and relatively to the considered following established differential equations indicated by the system (32), the LCLC filter can be represented by the following state equations (33):

$$\begin{bmatrix} \dot{i}_{L3} \\ \dot{i}_{L4} \\ \dot{v}_{C3} \\ \dot{v}_{C4} \end{bmatrix} = \begin{bmatrix} 0 & 0 & -\frac{1}{L_3} & 0 \\ 0 & 0 & \frac{1}{L_4} & -\frac{1}{L_4} \\ \frac{1}{C_3} & -\frac{1}{C_3} & 0 & 0 \\ 0 & \frac{1}{C_4} & 0 & -\frac{1}{R_{Load}C_4} \end{bmatrix} \begin{bmatrix} i_{L3} \\ i_{L4} \\ v_{C3} \\ v_{C4} \end{bmatrix} + \begin{bmatrix} \frac{1}{L_3} \\ 0 \\ 0 \\ 0 \end{bmatrix} v_{rec} \tag{33}$$

3. THE HYBRID SYSTEM CONTROL

3.1. The SEIG Control

The SEIG control strategy developed in this work is proposed and used in order to maintain the DC-bus voltage V_{dc} constant and equal to a desired reference voltage V_{dcref} .

With considering the fact that the obtained DC-bus voltage V_{dc} depend on the mechanical speed of the diesel engine coupled to the rotor of the SEIG and the DC-load current, the proposed control scheme includes a PI voltage regulator and a fuel flow controller as indicated by figure 1.

The PI voltage regulator is associated to a fuel flow controller in order to regulate the speed of the diesel engine by adjusting the fuel flow with the controlled governor.

3.2. The Buck converter and the PV control

The adaptation principle between the output panel voltage and the DC load voltage is based on the automatic adjustment of the buck converter duty cycle (α) indicated by relation (34) at the proper value to obtain the desired voltage and based on PWM principle.

$$V_{dc} = \alpha V_{panel} \tag{34}$$

4. SIMULATION RESULTS

4.1. Analyzes of the diesel engine/generator

The simulation in this work has been developed in Matlab/Simulink environnement.

The command of the diesel engine-SEIG system is based on the DC voltage required by the load equal to 560 V. This value is computed as a reference DC-bus voltage term.

Figure 7 gives the obtained output DC-bus voltage (pu) related to relation (31).

Figure 8 shows the voltage waveform v_s (pu) of the SEIG stator phase including the transient self-excitation process. The generated voltage grows and reaches the rated value.

Figure 9 gives the output rectifier voltage that result from a three sinusoidal signal rectified by full bridge 6 diodes rectifier.

Figure 10 gives the evolution of the diesel engine speed that reaches the nominal value at the steady state.

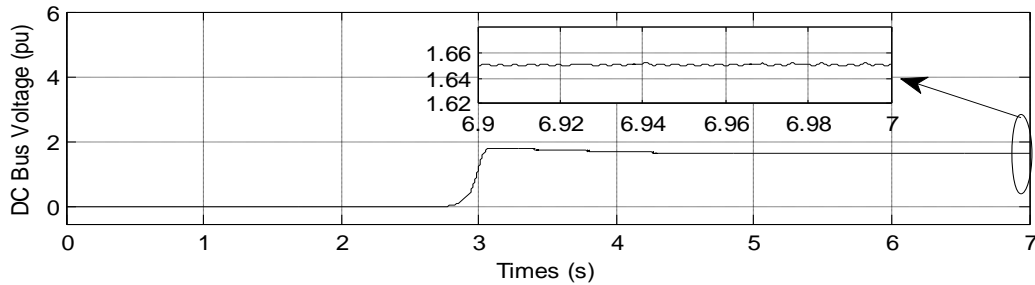


Figure 7. DC Bus voltage

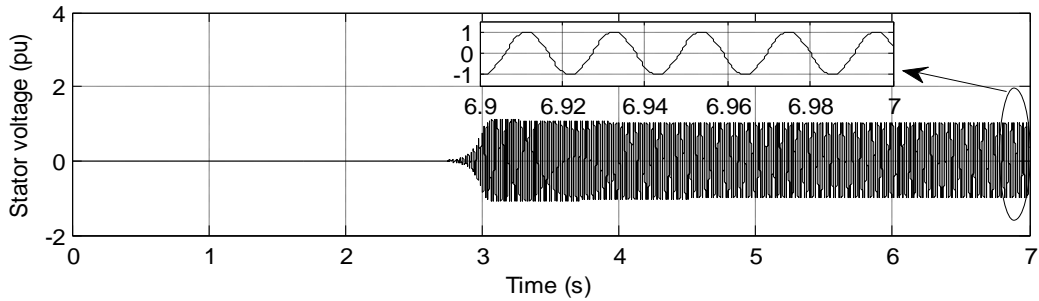


Figure 8. Stator SEIG voltage

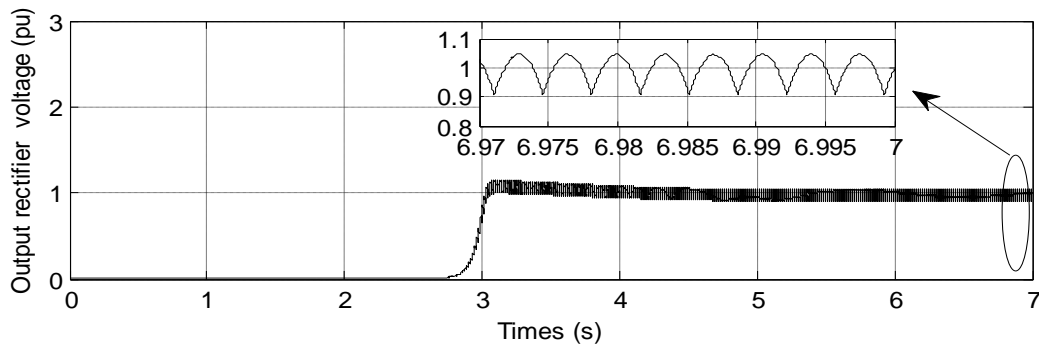


Figure 9. Output rectifier voltage

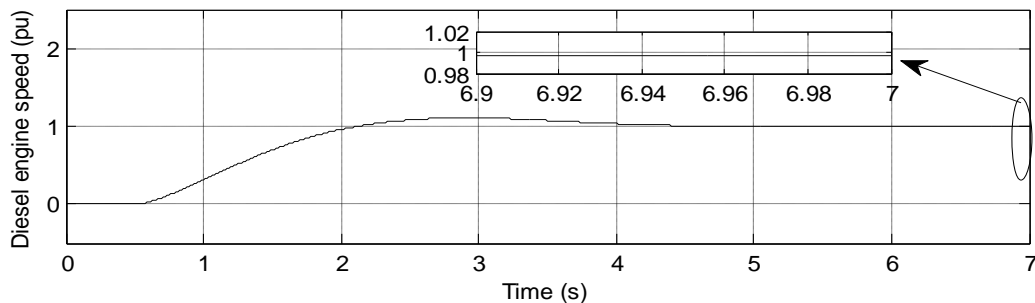


Figure 10. Diesel engine speed

4.2 Analyzes physical sizes relating to the photovoltaic panel and the buck converter

The command of the buck converter is based on the DC voltage required by the load equal to 560 V. This value is computed as a reference buck voltage term. The figures 11 and 12 give respectively the panel’s and the output buck converter voltages. The second one (figure 12) converges towards the required DC voltage according to the first one. With consider the rated DC load current as a base value, figure 13, figure 14 and figure 15 give respectively the panel current (pu), The capacitance C1 current (pu) and The inductance L2 current (pu). These figures show that panel current is perfectly continuous with a good choice of the capacitance value relatively to that of the inductance. The alternative current component of the inductance current is absorbed through the capacitance.

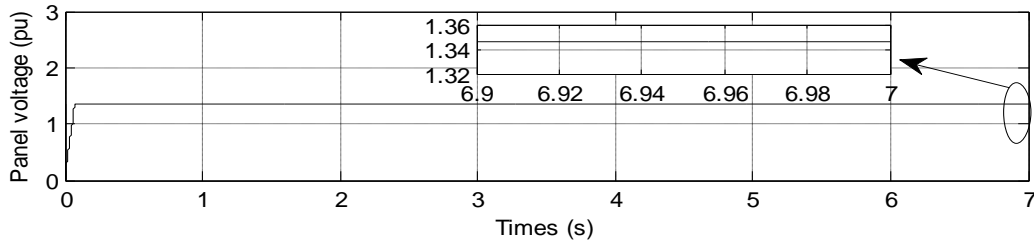


Figure 11. The panel voltage

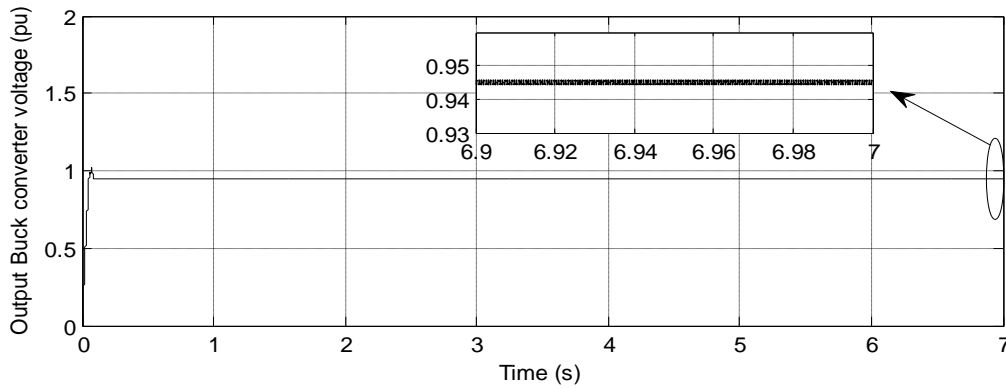


Figure 12. Output buck converter voltage

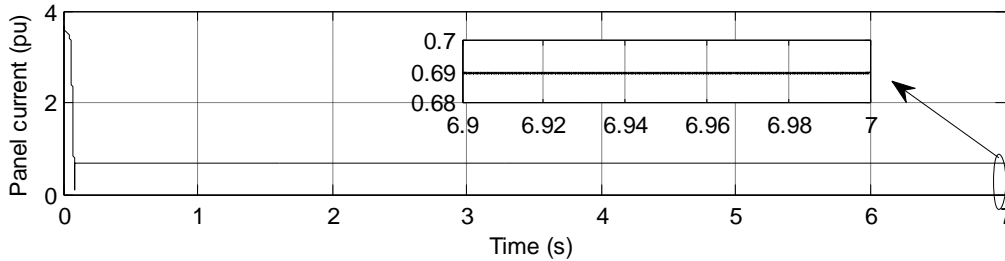


Figure 13. The panel current (pu)

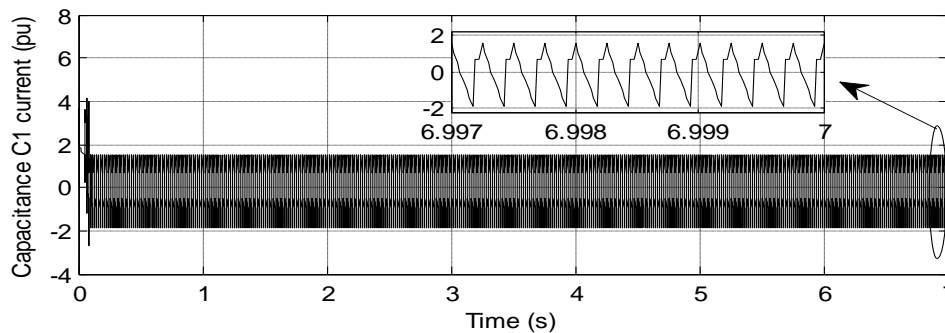


Figure 14. The capacitance C1 current (pu)

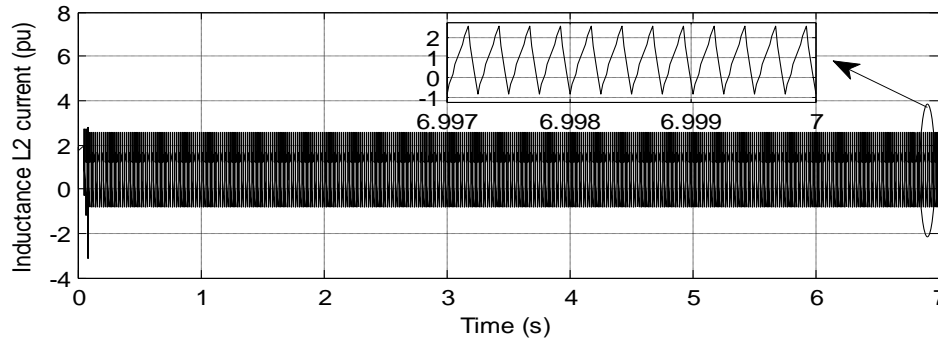


Figure 15. The inductance L2 current (pu)

5. CONCLUSION

The work here presented leads to the development of an overall dynamic model for a controlled PV-diesel structure scheme. Their stand alone challenge has been studied and focusing on the global system power management and coordination of systems supervision. Diesel engine coupled to a Self excited induction generator has been found suitable for remote area application and for energy saving a PV array was added. A conventional is sufficiently enough for the shaft speed regulation. The mutual exchange of information between the PV and diesel control output power bring up the system efficiency, a supervisor is used in the context.

Appendix

Table 1. SEIG Parameters

Rated power P_N	3.6 Kw
Rated voltage V_{sN}	240 V
Rated current I_N	7.8 A
Rated speed Ω_N	157 rad / s
Pole pairs p	4
Rotor resistance R_r	2.74 Ω
Stator resistance R_s	1.66 Ω
Stator inductance L_s	265.4 mH
Rotor inductance L_r	265.4 mH

Table 2. Parameters of Pv Cell (Polly-crystalline silicon)

Open circuit voltage: V_{oc}	0.6058 V
Short circuit current : I_{sc}	8.1 A
Parallel cell's resistance: R_{pc}	0.833 Ω
Series cell's resistance: R_{sc}	0.0833 m Ω
Solar cell's ideal factor : k	1.450
reverse diode saturation current I_{rs}	3.047e-7 A
Short circuit current temperature coefficient K_{SCT}	1.73e-3 A/ $^{\circ}K$
Reference cell's temperature: T_{c_ref}	25 $^{\circ}C$
Boltzmann's constant: β	1.38e-23
Band gap energy: E_g	1.11 eV

Table 3. Parameters of Pv module

Rated output power	216W
Open circuit voltage: V_{oc}	36.35 V
Number of series cells: n_s	60

Table 4. PV Array Parameters

Open circuit voltage: V_{oc}	509 V
Short circuit current : I_{sc}	8.1 A
Number of series modules: N_s	14
Number of parallel modules: N_p	5

Table 5. Diesel engine Parameters

Actuator gain constant k_g	1
Actuator time constant τ_g (s)	0.125
Engine torque constant k_{de}	1.15
Engine delay time τ_{de} (s)	0.5
Plant and fly wheel acceleration $J(kg.m^2)$	0.3
Friction coefficient β (kg.m/s)	0.1

Table 6. Nomenclature

<p>G : Global insulation ($W/m2$), G_{ref} : Reference insulation ($W/m2$), I_{ph} : Light-generated current source (A), I_{ph_ref} : Reference Light-generated current source (A) I_{sc} : Short circuit current (A), I_{sc-ref} : Reference Short circuit current (A), I_p : Panel current (A), I_{rs} : Reverse diode saturation current (A), I_c : Cell current (A), T_c : Cell junction temperature ($^{\circ}C$), T_{c_ref} : Reference cell temperature ($^{\circ}C$), α : Buck converter duty cycle PWM signal, V_c : Cell voltage (V), V_p : Panel voltage (V), R_{pc} : Parallel cell resistance (Ω), R_{sc} : Series cell resistance (Ω), E_g : Band gap energy of the semiconductor (eV), K_{SCT} : Short circuit current temperature coefficient ($A/^{\circ}C$), k : Solar cell ideal factor (1.45), n_s : Number of series cells modules, N_s : Number of series modules, N_p : Number of parallel modules, q : Electron charge (1.6022e-19), T : Buck converter operating PWM signal period (s), β : Boltzman constant (1.3807e-23), C_{de} : Diesel engine torque, ϕ : Fuel flow, τ_{de} : Diesel engine delay time, k_g : Actuator gain constant,</p>	<p>τ_g : Actuator time constant, S_{gc} : Fuel flow control signal, v_{sd} : Direct stator voltage (V), v_{sq} : Quadratic stator voltage (V), v_s : Per phase stator voltage (V), v_{s1}, v_{s2}, v_{s3} : Per phase stator voltage, V_{dc} : DC-bus voltage, v_{rec} : Rectified voltage, i_{sd} : Direct stator current (A), i_{sq} : Quadratic Stator current (A) R_s : Stator resistance, R_r : Rotor resistance, L_s : Stator cyclic inductance, L_r : Rotor cyclic inductance, ℓ_s : Stator leakage inductance, ℓ_r : Rotor leakage inductance, M_{sr} : Magnetizing inductance ϕ_{ds} : Direct stator flux (Wb), ϕ_{qs} : Quadratic stator flux (Wb), ϕ_{dr} : Direct rotor flux (Wb), ϕ_{qr} : Quadratic rotor flux (Wb), ω_r : Electric rotor speed (rad/s), p : Machine pair pole number, C : Excitation capacitance, V_{cd} : Direct capacitor voltage, V_{cq} : Quadratic capacitor voltage,</p>
--	---

REFERENCES

- [1]. J.Faria, E.Margato, M.J. Resende, “asynchronous generator excited by current controlled voltage source inverter using rotor field oriented control”, *12th International Power electronics and motion control conference*, **1**, 224-229, (2006).
- [2]. T.senjyu, M.Data, A.Yona, C. H. Kim, “A control method for small utility connected large PV system to reduce Frequency deviation using a minimal –order observer”, *IEEE Energy conversion*, **24**, issue 1, 211-221, (2009).
- [3]. M.rached ,A.E.S.Kaddah, “New control approach for a PV-diesel autonomous power system”, *Science direct electric power system research*, **78**, issue 6, 949-956, (2008).
- [4]. M.Datta,T.Senjyu, A.Yona, “A coordinated control method for levelling PV output power fluctuation of PV-diesel hybrid system connected to isolated power utility”, *IEEE Energy conversion*, **24**, 153-162, (2009).
- [5]. A.Kishore, R.C.Prasad, B.M. Karan, “Matlab simulink based DQ modeling and dynamic characteristics of three phase self excited induction generator”, *Progress In electromagnetic research symposium*, Cambridge, USA. 26-29, (2006).
- [6]. M.L.Elhafyani, S.Zouggar, M.Benkaddour, Zidani, “Permanent and Dynamic Behaviours of Self-excited Induction Generator In balanced mode”, *Moroccan journal of condensed matter*, **7**, issue 13, (2006).
- [7]. F.juado, J.R.Saenz, “neuro fuzzy control for autonomous wind diesel system using biomass”, *Renewable energy*, **27**, 39-56, (2002).
- [8]. T.Bjzic, Z.Ban, I.Volaric, “Control of a Fuel Cell Stack loaded with DC/DC Boost Converter”, *Industrial Electronics. IEEE International Symposium*, 1489–1494, June 30-July.2, (2008).
- [9]. R. Chenni, M. Makhoulouf, T. Kerbache, A. Bouzid, “A detailed modeling method for photovoltaic cells”, *Energy*, **32**, 1724–1730, (2008).
- [10]. K.H. Chao, S.H. Ho, M.H. Wang, “Modeling and fault diagnosis of a photovoltaic system”, *Electric Power Systems Research*, **78**, 97–105, (2008).
- [11]. L.S.Kim, “Sliding mode controller for the single phase grid-connected photovoltaic system”, *Applied Energy*, **83**, 1101–1115, (2006).
- [12]. A.Saadi, A.Moussi, “ Optimisation of Buck-boost converter by MPPT Technique with a Variable Reference Voltage Applied to Photovoltaic Water Pumping System under Variable Weather condition”, *Asian Journal of Information Technology*, **6**, issue 2, 222-229, (2007).
- [13]. N.Hidouri, L.Sbita, “Water photovoltaic pumping system based on DTC SPMSM drives”, *JEETA*, **1**, 111-119, (2010).
- [14]. N.Hidouri, L.Sbita, “A new DTC SPMSM drive scheme for photovoltaic pumping system”, *IJSC*, **1**, 111-119, (2010).
- [15]. S.Hammadi, N. Hidouri, L. Sbita, “A DTC-PMSG-PMSM Drive Scheme for an Isolated Wind turbine water Pumping System”, *International Journal of Research and Reviews in Electrical and Computer Engineering (IJRRECE)*, **1**, issue 1, 1-6, (2011).
- [16]. T.Mhamdi, N.Hidouri, L.Sbita, “Hybrid Photovoltaic-Diesel System Control Scheme for an Isolated Grid”, *Science Academy Transactions on Renewable Energy Systems Engineering and Technology (SATRESET)*, **1**, issue 1, 1-10, (2011).
- [17]. V.M.Pereira, J.A.Pomilio, P.A.V.Ferreira, “Induction generator driven by internal combustion engine with voltage and frequency regulation”, *IEEE International Symposium on Industrial Electronics*, **3**, 834-839, (2002).
- [18]. D.Canever, G.J.W.Dudgeon, S.Mascusso, J.R.Mc.Donald, F.Silvestro, “Model validation and coordinated operation of a photovoltaic array and diesel power plant for distributed generation”, *Power Engineering Society Summer Meeting IEEE*, **1**, 626-631, (2001).
- [19]. G.V. Jayaramaiah, B.G. Fernandes, “Novel maximum power point tracker for stand-Alone self-Excited induction generator”, *Proceedings of India International Conference on Power Electronics*, 105-110, (2006).
- [20]. Y.Kumsuwan, W.Srirattanawichaikul, S.Permrudeepreechacharn, “Matlab/simulink based on $\alpha\beta$ modeling of self excited induction generator”, *EENET*, (2008).
- [21]. D.Seyoum, C.Grantham and F.Rahman, “Improved flux estimation in induction machines for control application”, *Journal of Electrical and Electronic Engineering Australia (JEEEA)*, **22**, issue 3, 243-248, (2003).
- [22]. A.Toumi, M.Ghariani, I.B.Salah, R.Neji, “Three-phase PFC rectifier using a switching current injection device for vehicle power train application”, *International renewable energy congress*, 417-420, (2010).
- [23]. S.Gao, S.S.Murthy, G.Bhuvaneswari, M.S.L.Garyathri, “Design of microcontroller based electronic load controller for a self excited induction generator supplying single –phase loads”, *journal of power electronics*, **10**, issue 40, 444-449, (2010).
- [24]. A.M. Sharaf, E.S. Abdin, “A digital Simulation Model for Wind-Diesel Conversion scheme”, *IEEE System Theory, 1989. Proceedings*, 160-166, (1989).
- [25]. T.Ouchbel, S.Zouggar, M.Sedik, M. Oukili, M. Elhafyani, A.Rabhi, “Control of the excitation reactive power of asynchronous wind turbine with variable speed”, *International renewable energy congress*, 242-249, (2010).
- [26]. D. Seyoum, C.Grantham and F.Rahman, “Analyssis of an isolated induction generator driven by a variable speed prime mover”, *international conference of power electronics*, **487**, 580-585, (2002).